Dust Deposition Near an Eroding Source Field[†]

L. J. Hagen,[1]* S. Van Pelt,[2] T. M. Zobeck[3] and A. Retta[1]

[1] *USDA-ARS, GMPRC, Manhattan, KS, USA*
[2] *USDA-ARS, Big Spring, TX, USA*
[3] *USDA-ARS, Lubbock, TX, USA*

Correspondence to: L. J. Hagen, Research Associate, KS State University, GMPRC, 1515 College Avenue, Manhattan, KS 66502, USA. E-mail: hagen@weru.ksu.edu
Contribution from USDA, ARS in cooperation with Kansas Agricultural Experiment Station. Contribution No. 05-219-J from the Kansas Agricultural Experiment Station, Manhattan, KS.
[†]This article is a U.S. Government work and is in the public domain in the USA.

Abstract

Deposition of suspended dust near eroding source fields can have detrimental effects on vegetation, as well as on soil and water quality. This study was undertaken to quantify dust deposition within 200 m of a source field during wind erosion events. Erosion was measured with BSNE samplers on a small field of Amarillo fine sandy loam at field at Big Spring, TX. Suspension-sized dust discharge averaged 33 ± 5 per cent of the total sediment discharge and ranged from 18.0 to 147.4 kg m^{-1} during eight selected storm events. Within 200 m of the source field boundary, dust collected in deposition samplers placed above a vegetated surface averaged 34 per cent of initial dust discharge. Predicted deposition, according to a line source model, was 43 per cent. Actual deposition was likely near that predicted, because of lateral diffusion of the dust and some under-sampling by the disk samplers. Thus, the line source model seems useful in estimating both the pattern and quantity of deposition. About 30 per cent of the suspended dust was deposited within the initial 50 m of vegetated surface, but only about 12–15 per cent was deposited in the initial 10 m. Published in 2006 by John Wiley & Sons, Ltd.

Keywords: deposition; dust; wind erosion

Offsite costs generally far exceed onsite costs from wind erosion (Huszar, 1989; Pimentel *et al*., 1995; Piper and Huszar, 1989). Hence, it is becoming increasingly important to design onsite wind erosion controls to limit detrimental offsite impacts. In general, there are three major offsite damage zones. These include the near-field (<200 m) and far-field (>200 m) zones where deposition of suspended dust occurs, as well as stable areas where aggregates moving by saltation and creep (hopping and rolling aggregates) are trapped near erodible field boundaries. The proportion of soil moving as suspension or saltation/creep varies widely with soil texture, field scale and surface conditions. Thus, emerging wind erosion models, such as the Wind Erosion Prediction System (WEPS) (Wagner, 1996; Hagen, 2001, 2004), that predict the separate components of suspension and saltation/creep of soil crossing each boundary of an eroding field allow for greatly improved analyses of potential offsite impacts from a given field.

Offsite concentrations of far-field dust have been reported (Claiborn *et al*., 2000; Draxler *et al*., 2001), along with the deposition rates (Reheis, 2003; Reheis and Kihl, 1995; Li *et al*., 2004). Studies on loess thickness also provide long-term data on far-field dust deposition (Frazee *et al*., 1970; Mason, 2001). More information is needed, however, to quantify dynamics of the near-field dust, because it contributes relatively large amounts of deposition per unit of downwind area. Dust contaminants may damage vegetation (Reheis, 1997), as well as degrading water and soil quality upon deposition. It also severely reduces both visibility (Wagner and Hagen, 2001) and air quality during transit (Saxton *et al*., 2000).

Near-source deposition of fine dust also creates another problem. This deposition depletes the dust available for long-range transport (Etyemezian *et al*., 2004) and, thus, causes large differences between measured downwind ambient concentrations and regional model results that rely on source emission estimates (Watson and Chow, 2000). Improved factors to estimate near-source capture efficiency (CF) of particulate matter of less than 10 μm aerodynamic diameter (PM10) from various dust sources such as unpaved roads and agricultural tilling have recently been proposed for use in the United States (Pace, 2005). The CFs range from 0 to 10 per cent for barren lands, from 10 to 40 per cent for grass and shrub cover and from 80 to 100 per cent for forest. The CF values of fugitive

PM10 generated during wind erosion are believed to be less than those cited and hence are not recommended for use with wind-generated PM10 (Pace, 2005). Data are currently lacking to quantify the near-source CF for wind erosion events.

The objectives of this study were to determine for the near-field (0–200 m) zone (a) fraction of suspended dust deposited, (b) size distribution of the deposited dust and (c) utility of a line-source theoretical diffusion–deposition model for prediction of near-field dust deposition.

Methods and Materials

Field layout and instrumentation

An erodible, circular field 182 m in diameter was chiseled, planed smooth, and maintained in a bare condition at Big Spring, TX. The field was instrumented with clusters of BSNE sediment samplers (Fryrear, 1986) and meteorological sensors including saltation impact sensors (Sensits) (Figure 1). The BSNE clusters consisted of passive sediment samplers located at 0·05, 0·10, 0·20, 0·5 and 1·0 m above the soil surface (Figure 2). These samplers trapped the horizontal soil flux. Wind direction was measured at the center of the field with a wind vane at 2 m height, and cup anemometers at 0·5 and 2·0 m heights measured wind speed. The soil is classified as an Amarillo fine sandy loam, and the surface layer was 84 per cent sand, 8 per cent silt, 8 per cent clay and 0·3 per cent organic matter.

In the first year of the study, 2002, the deposition area surrounding the source field was sown to a low population of barley (*Hordeum vulgare* L.), which increased in height from 0·35 ± 0·05 to 0·5 ± 0·05 m during the storm events. In the second year, 2003, it was sown to a low population of triticale (*Trifcosecale rimpaui* Wittm.), which increased in height from 0·25 ± 0·05 to 0·5 ± 0·15 m during the storm events. The vegetation did not provide a closed canopy during the storm events.

Twelve dust deposition samplers (Figure 3) were placed along three of the most probable downwind transects (Figure 1) from the erodible field. Transects were selected based on past observations of local dust storm tracks. The deposition samplers were constructed from commercial inverted flying disks, 245 mm internal diameter and 34 mm deep. To retard dust blowout, a porous mat (3 mm openings) covered by a screen (0·3 mm openings) was placed in the bottom of each disk. The deposition samplers were tested for dust blowout in a laboratory wind tunnel (Figure 4). The test dust had a size range of 2–100 μm diameter. The overall sampling efficiency of the deposition samplers under field conditions is unknown, but prior wind tunnel tests show that it generally decreases with wind speed but increases with turbulence level (Hall and Upton, 1988). Hence, the deposition samplers were mounted in the low-wind-speed, high-turbulence region slightly above the vegetation and were moved up as the vegetation height increased.
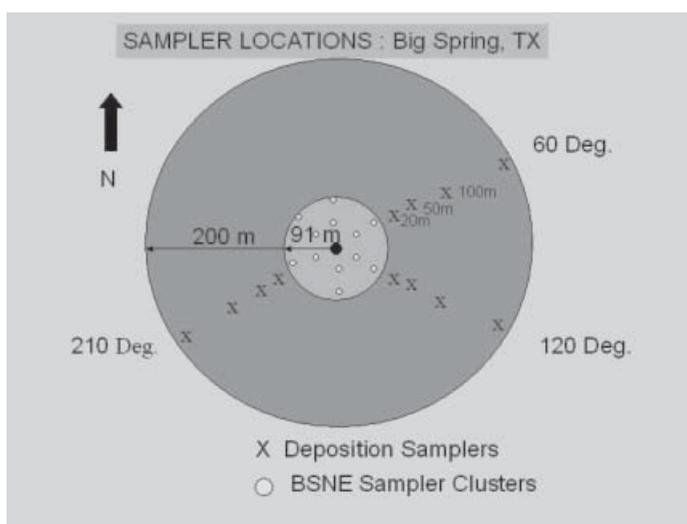
Figure 1. Schematic diagram of eroding, circular source field (91 m radius) with BSNE sampler locations and surrounding deposition area (200 m) with flying-disk deposition sampler locations.
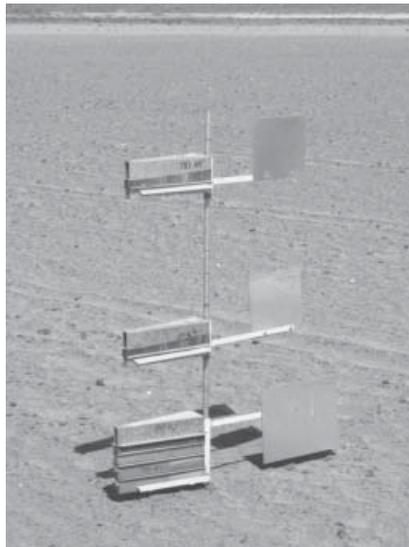
Figure 2. One of 13 clusters of BSNE sediment samplers installed on eroding source field.

Figure 3. One of 12 flying-disk sediment samplers that were mounted in a framework used to adjust sampler height as vegetation height increased. This figure is available in colour online at www.interscience.wiley.com/journal/espl
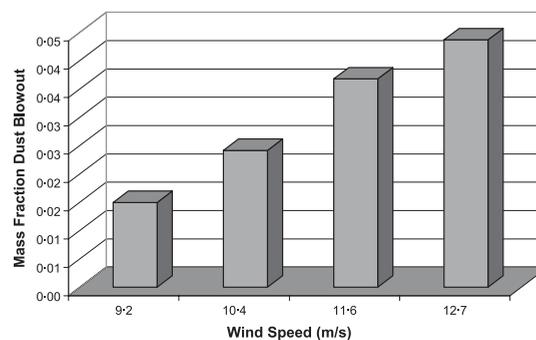
Figure 4. Wind tunnel blowout tests of flying-disk deposition samplers, showing less than 5 per cent sediment blowout over the range of test wind speeds.
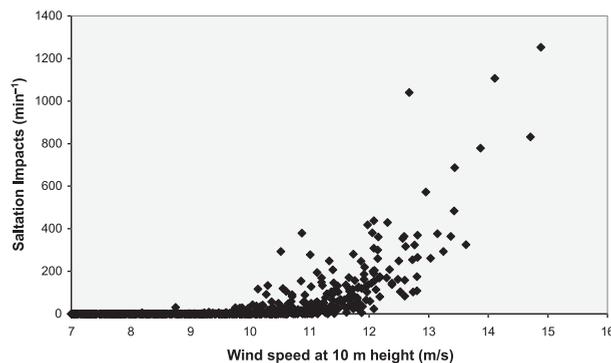
Figure 5. Typical storm event (17 March 2003) illustrating counts of saltating aggregate impacts on Sensit as a function of wind speed.

Data analysis procedures

Eight dust storms during 2002 and 2003 that had wind directions within ±17° of a sampler transect were selected for analysis. The eroding field surface was relatively smooth and the wind speed profiles were used to estimate aerodynamic roughness (Z_0) that ranged from 0·3 to 0·6 mm. The Z_0 values were then used in the log-law wind speed profile to estimate wind speeds at the 10 m height that is typically used for reporting surface wind speeds. To classify the storms for the diffusion model, a representative wind speed for each storm event was determined by weighting one-minute average wind speeds by the corresponding Sensit counts. The weighting method assumes that the dust flux increases in proportion to saltation flux (Saxton *et al.*, 2000). The representative wind speeds ranged from 9·7 to 12·8 m s^{-1} with an average of 11·6 m s^{-1}. The Sensit counts for a typical storm event show that the threshold wind speed needed to initiate erosion was between 9·5 and 10·0 m s^{-1} (Figure 5).

After each storm, dry weights of soil samples in the BSNE samplers were recorded, and the horizontal sediment passage at each BSNE cluster was determined by fitting empirical equations (Fryrear *et al.*, 1991) to the sediment flux and then integrating from the surface to a height of 2 m to determine sediment discharge passing each cluster. In this study, TableCurve software (SPSS, 2000) was applied using the least-squares criterion to determine coefficients for fitting equations to data. Mathcad software (Mathsoft, 2003) was used to perform numerical integrations of various equations.

To determine sediment discharge from the field, a power equation was fitted to individual cluster discharge data

$$Q_t = ax^b \tag{1}$$

where Q_t is total discharge (kg m^{-1}), x is downwind distance (m) from the upwind field boundary and the fitting coefficients are a and b.

The fraction of suspension-size dust in the BSNE discharge was also determined. We assumed that aggregates less than 100 μm in diameter were suspended and estimated their proportions in the horizontal flux as 1·0, 0·91 and 0·40 at heights of 1·0, 0·5 and 0·22 m, respectively. These estimates were based on size distributions obtained from micromesh sieving of sediment collected in the BSNE samplers during several prior storms on the same field. By using the preceding heights, vertical profiles of catch in several of the downwind clusters were fitted to an empirical power equation and then integrated from the surface to 2 m as

$$Q_s = \int_{0\cdot05}^{2\cdot0} c\, Z^d \mathrm{d}Z + \int_0^{0\cdot05} c\, 0\cdot05^d \mathrm{d}Z \tag{2}$$

where Q_s is horizontal suspended dust discharge (kg m^{-1}), Z is height above the surface (m) and c and d are fitting coefficients. Because of the high near-surface turbulence levels, the horizontal dust discharge was assumed constant in the $0\cdot0 - 0\cdot05$ m layer.

After each storm, the sediment in the flying-disk deposition samplers was collected, dried, sieved with micromesh sieves and weighed. An exponential equation was fitted to the deposited soil catch as

$$P = f \exp(gx + hx^2) \tag{3}$$

where P is deposition (kg m^{-2}), x is downwind distance from the eroding field boundary and f, g and h are fitting coefficients. The preceding equation was integrated from 0 to 200 m to determine the cumulative near-field sediment deposition (kg) along given transects of samplers.

For comparison of the measured deposition data with theoretical predictions, we used a line-source diffusion–deposition model (Huang, 1999). This model was selected because it is derived from the fundamental equations governing the particle diffusion processes where mass is conserved. For particle concentration near the surface, the model solution has the form

$$X = Q\frac{(1 + p)}{hu_h\Gamma(1 - v)}\exp\left(-\frac{h^v u_h}{(1 + p)^2 K_h x}\right)\left(\frac{h^2 u_h}{(1 + p)^2 K_h x}\right)^{(1 - v)} \tag{4}$$

$$D = XV_S \tag{5}$$

where the sediment concentration, X (kg m^{-3}), multiplied by sediment fall velocity, V_S (m s^{-1}), is equal to the deposition rate per unit area, D (kg m^{-2} s^{-1}), for a mass emission rate from the source Q (kg m^{-1} s^{-1}) at the downwind distance x (m). The line source is located at the downwind boundary of the source field with wind speed u_h at height h (m) above the surface, and Γ is the gamma function. The eddy diffusivity K_h (m^2 s^{-1}) is estimated as

$$K_h = ku_* h \tag{6}$$

and the parameter

$$v = -\frac{V_S}{(1 + p)ku_*} \tag{7}$$

where k is the von Karman constant (about 0·4), p is the exponent for the power-law wind speed profile (for this case about 0·23) and u_* (m s^{-1}) is friction velocity over the deposition region. The fall velocity in air, V_S (m s^{-1}), for sediment aggregates of size S (μm), was estimated from data given by Royco Instruments (1974) using the empirical equation

$$V_S = \exp(-9·261 + 1·850 \ln(S))(\rho/2·0) \tag{8}$$

where ρ (Mg m^{-3}) is aggregate density.

Results and Discussion

Suspension-sized dust discharge leaving the downwind edge of the eroding field averaged 33 ± 5 per cent of the total sediment discharge trapped by the BSNE samplers. The correlation between fraction of suspension-sized dust in individual storms and total storm discharge was low ($R^2 = 0·2$). Suspension-sized discharge ranged from 18·0 to 147·4 kg m^{-1} during the eight storm events, with an average of 89·6 kg m^{-1}. The field length in this study, up to 180 m, was relatively short compared with that of typical agricultural fields. However, prior analysis (Hagen *et al*., 1999) and measurement (Gillette *et al*., 1997) of sediment generation by wind have shown that the proportion of suspended dust in the total discharge over a source area generally increases with increasing distance from a non-erodible upwind boundary.

The mass distribution among size classes of sediment deposited in samplers over the vegetated surface was dominated by aggregates more than 30 μm in diameter (Figure 6). Because of differing fall velocities, the proportion of coarse sediment greater than 75 μm in diameter in the deposited sediment decreased with distance downwind, whereas the proportion of fine sediment less than 10 μm increased.

The model equations were implemented using an Excel spreadsheet (Microsoft, 1999). The theoretical deposition using Equations (4)–(8) provides a steady-state solution from a line source at a given height for specific sediment sizes. However, the suspended discharge from the field occurs over a limited height with unsteady winds, for a range of sediment sizes. Preliminary tests using various wind speeds showed relatively small differences in near-field deposition rates in response to the choice of erosive wind speeds between 10 and 15 m s^{-1} at a height of 10 m. This occurred primarily because increasing wind speeds increased both rate of horizontal movement across the surface and rate of particle diffusion to the surface.
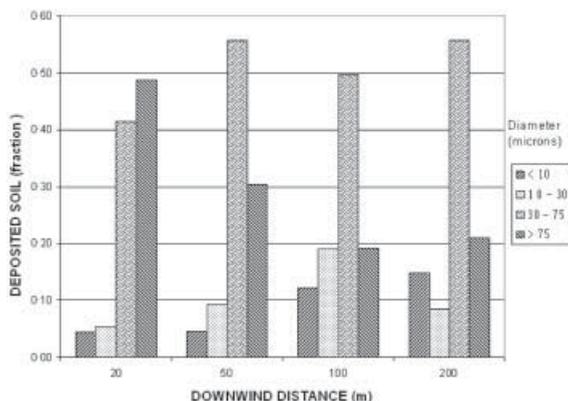
Figure 6. Variations in aggregate size classes of deposited dust mass with downwind distance.

Table I. Estimated parameters used for theoretical prediction of downwind deposition with source height of 0·35 m

Aggregate class range (µm)	Selected aggregate diameter (µm)	Aggregate density (Mg m⁻³)	Settling velocity (m s⁻¹)	Wind speed at 10 m (m s⁻¹)	Aerodynamic roughness (m)
<10	7	2·0	0·003	12	0·02
10–30	25	1·8	0·033	12	0·02
30–75	47	1·7	0·100	12	0·02
>75	85	1·6	0·282	12	0·02
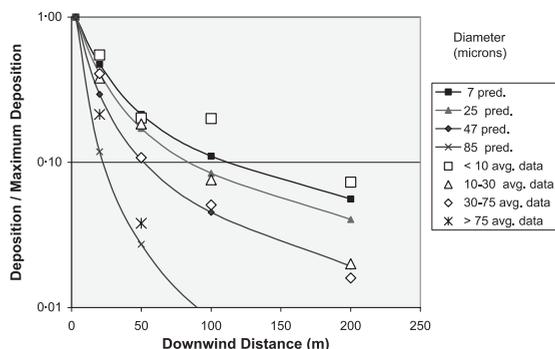
Figure 7. Predicted (solid lines) and average measured (open symbols) deposition patterns for various suspended sediment diameters.

Average parameters (Table I) for the theoretical equations for eight storm events were estimated from both storm wind data and surface conditions in the deposition area. Theoretical and measured sediment deposition was compared in two ways. First, the patterns of deposition for various size classes were compared with the theoretical deposition patterns. The patterns were obtained by dividing both the theoretical and measured deposition by their respective maxima (Figure 7). Because the height of the line emission source was selected as 0·35 m, the maximum theoretical deposition occurred at about 3 m downwind. Overall, the mean measured deposition and the theoretical deposition patterns were in good agreement, with a coefficient of determination (R^2) of 0·98. This result suggests that the estimated parameters for the theoretical equations are valid.

In the second comparison, the mean and standard deviation of the cumulative fraction of measured deposition were determined, along with the cumulative theoretical deposition (Figure 8). For the theoretical computation we assumed a log-normal distribution of the suspended discharge with 12, 26, 37 and 25 per cent in the <10, 10–30, 30–75 and >75 µm size classes, respectively. Within 200 m of the eroding field, the deposition fraction of total suspended discharge averaged 34 per cent for measured deposition and 43 per cent for the theoretical deposition. The consistent
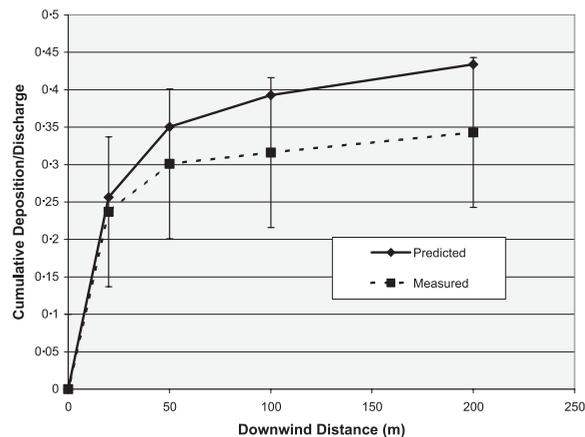
Figure 8. Measured (mean and standard deviation) and predicted cumulative fractions of deposition of suspended sediment discharge from an eroding source field.

increase in difference between theoretical and measured deposition in the downwind direction is likely caused by both lateral diffusion of sediment leaving the source field and some under-sampling of the finest aggregates by the deposition samplers. As discussed by Goossens (2005), samplers only measure dust accumulation, while models generally predict deposition.

Most of the near-field dust deposition occurred within 50 m of the eroding field, but significant amounts of dust deposition would bypass buffer strips 10 m in width. The variance in measured deposition among storms (Figure 8) was likely caused by variations in atmospheric conditions, as well as by changes in the vegetation composition and height over the two seasons.

Summary and Conclusions

Deposition of suspended sediments near eroding source fields can have detrimental effects on vegetation, as well as on soil and water quality. This study was undertaken to determine quantitative estimates of the size distribution, pattern and magnitude of the near-source sediment deposition during wind erosion events.

Wind erosion during 2002 and 2003 was measured with BSNE samplers on a circular 180 m diameter, fine sandy loam field at Big Spring, TX. The suspension-sized sediment discharge leaving the downwind edge of the eroding field averaged 33 ± 5 per cent of the total sediment discharge. At the maximum eroding field length, suspension-sized discharge averaged 89·6 kg m^{-1} and ranged from 18·0 to 147·4 kg m^{-1} during eight selected storm events.

Within 200 m of the source field boundary, deposition of suspended sediment on a nonerodible, vegetated surface was substantial. Samples collected in flying-disk samplers showed deposition was about 34 per cent of the initial suspension discharge. Predicted deposition, according to a line source model, was 43 per cent. It is likely that the actual deposition was close to the predicted value, because of lateral diffusion of the sediment and because of some under-sampling by the disk samplers. Thus, the line source deposition model seems useful to predict both the pattern and magnitude of deposition. However, good estimates of both the magnitude and size distribution of the suspended discharge from the source are needed for accurate results.

Total suspension-sized dust deposition was near the upper range, 0·4, of capture efficiencies of fine dust suggested for grasslands, but the deposition patterns in this study showed reduced deposition of the fine dust. Hence, our results support the suggestion of Pace (2005) that capture efficiencies of dust subject to long-range transport will be decreased for erosive wind speed conditions.

The observed deposition amounts decreased at an exponential rate downwind from the vegetated boundary. This trend agrees with both theory and the loess depths observed near forest boundaries (Tsoar and Pye, 1987).

About 30 per cent of the suspended sediment was deposited within the initial 50 m of vegetated surface, but only about 12–15 per cent was deposited in the initial 10 m. Hence, typical 10 m wide grass buffers may not protect critical downwind areas from significant deposition during wind erosion events. Additional measured data are needed for a range of soil types, field scales and deposition surfaces to further validate the model for prediction of near-source deposition.

Acknowledgements

References

Claiborn C, Finn D, Larson T, Koenig J. 2000. Windblown dust contributes to high PM2·5 concentrations. *Journal of the Air and Waste Management Association* **55**: 1440–1445.

Draxler RR, Gillette DA, Kirkpatrick JS, Heller J. 2001. Estimating PM 10 air concentrations from dust storms in Iraq, Kuwait and Saudi Arabia. *Atmospheric Environment* **35**: 4315–4330.

Etyemezian V, Ahonen S, Nikolic D, Gillies J, Kuhns H, Gillette DA, Veranth J. 2004. Deposition and removal of fugitive dust in the arid southwestern United States: measurements and model results. *Journal of the Air and Waste Management Association* **54**: 1099–1111.

Frazee CJ, Fehrenbacher JB, Krumbein WC. 1970. Loess distribution from a source. *Soil Science Society of America Proceedings* **34**: 296–301.

Fryrear DW. 1986. A field dust sampler. *Journal of Soil and Water Conservation* **41**(2): 117–120.

Fryrear DW, Stout JE, Hagen LJ, Vories ED. 1991. Wind erosion: field measurement and analysis. *Transactions of American Society of Agricultural Engineers* **34**(1): 155–160.

Gillette DA, Fryrear DW, Gill TE, Ley T, Cahill TA, Gearhart EA. 1997. Relation of vertical flux of particles smaller than 10 microns to total aeolian horizontal mass flux at Owens Lake. *Journal of Geophysical Research* **102**(D22): 26009–26015.

Goossens D. 2005. Quantification of the dry Aeolian deposition of dust on horizontal surfaces: an experimental comparison of theory and measurements. *Sedimentology* **52**: 859–873.

Hagen LJ. 2001. Validation of the Wind Erosion Prediction System (WEPS) erosion submodel on small cropland fields. Proceedings of International Symposium on Soil Erosion Research for the 21st Century, Honolulu, HI, 2001. *American Society of Agricultural Engineers'* 479–482.

Hagen LJ. 2004. Evaluation of the Wind Erosion Prediction System (WEPS) erosion submodel on cropland fields. *Environmental Modeling and Software* **19**: 171–176.

Hagen LJ, Wagner LE, Skidmore EL. 1999. Analytical solutions and sensitivity analyses for sediment transport in WEPS. *Transactions of the American Society of Agricultural Engineers* **42**(6): 1715–1721.

Hall DJ, Upton SL. 1988. A wind tunnel study of the particle collection efficiency of an inverted frisbee used as a dust deposition gage. *Atmospheric Environment* **22**(7): 1383–1394.

Huang CH. 1999. On solutions of the diffusion–deposition equation for point sources in turbulent shear flow. *Journal of Applied Meteorology* **38**: 250–254.

Huszar PC. 1989. Targeting wind erosion reduction measures based upon off-site costs. *Journal of Soil and Water Conservation Society* **44**(6): 612–615.

Li F-R, Zhao L-Y, Zhang H, Zhang T-H, Shirato Y. 2004. Wind erosion and airborne dust deposition in farmland during spring in the Horqin Sandy Land of eastern Inner Mongolia, China. *Soil and Tillage Research* **75**: 121–130.

Mason JA. 2001. Transport direction of Peoria Loess in Nebraska and implications for loess sources in the central Great Plains. *Quaternary Research* **56**: 79–86.

Mathsoft. 2003. *Mathcad* Version 11.2a. Mathsoft: Cambridge, MA.

Microsoft. 1999. *Excel 2000*. Microsoft: Redmond, WA.

Pace TG. 2005. *Methodology to Estimate the Transportable Fraction (TF) of Fugitive Dust Emissions for Regional and Urban Scale Air Quality Analyses* (8/3/2005 revision). http://www.epa.gov/ttn/chief/emch/invent/transprotable_fraction_080305_rev.pdf [accessed 7 June 2006].

Pimentel D, Harvey P, Resosudarmo P, Sinclair K, Kurz D, McNair M, Crist S, Shpritz L, Fitton L, Saffouri R, Blair R. 1995. Environmental and economic costs of soil erosion and conservation benefits. *Science* **267**: 1117–1123.

Piper SL, Huszar PC. 1989. Re-examination of the offsite costs from wind erosion in New. Mexico. *Journal of Soil and Water Conservation* **44**(4): 332–334.

Reheis MC. 1997. Dust deposition downwind of Owens (dry) Lake, 1991–1994: preliminary findings. *Journal of Geophysical Research* **102**(D22): 25999–26008.

Reheis MC. 2003. *Dust Deposition in Nevada, California, and Utah, 1894–2002* US Geological Survey Open-File Report 03-138. http://pubs.usgs.gov/of/2003/ofr-03-138/ [accessed 7 June 2006].

Reheis MC, Kihl R. 1995. Dust deposition in southern Nevada and California, 1984–1989: relations to climate, source area, and source lithology. *Journal of Geophysical Research* **100**(D5): 8893–8918.

Royco Instruments. 1974. *Characteristics of Particles and Particle Dispersoids*. Royco Instruments: Menlo Park, CA.

Saxton K, Chandler D, Stetler L, Lamb B, Claiborn C, Lee BH. 2000. Wind erosion and fugitive dust fluxes on agricultural lands in the Pacific Northwest. *Transactions of American Society of Agricultural Engineers* **43**: 623–630.

SPSS. 2000. *TableCurve 2D*, Version 5.0. SYSTAT Software: Richmond, CA.

Tsoar H, Pye K. 1987. Dust transport and the question of desert loess formation. *Sedimentology* **34**: 139–153.

Wagner LE. 1996. An overview of the Wind Erosion Prediction System. In *International Conference on Air Pollution from Agricultural Operations*, Kansas City, MO, 1996, Conference Proceedings. Midwest Plan Service: Ames, IA; 73–78.

Wagner LE, Hagen LJ. 2001. Application of WEPS generated soil loss components to assess off-site impacts. In *Sustaining the Global Farm*, Proc of 10th International Soil Conservation Organization Conference, 1999, Stott DE, Mohtar RH, Steinhardt GC (eds). Purdue University: West Lafayette, IN; 935–939.

Watson JG, Chow J. 2000. *Reconciling Urban Fugitive Dust Emissions Inventory and Ambient Source Contribution Estimates*, Desert Research Institute Report 6110.4F, prepared for US EPA, Research Triangle Park, NC.